Thermochimica Acta, 28 (1979) 175–184

THE FORMATION OF PORTLAND CEMENT CLINKER UNDER APPLIED ELECTRIC FIELDS. II. THEORY AND MECHANISM OF THE THERMAL REACTION SEQUENCE

K. J. D. MACKENZIE
Chemistry Division, D.S.I.R., Private Bag, Petone (New Zealand)
(Received 17 February 1978)

ABSTRACT

Theoretical considerations of the effects of electric fields on the solid-state reactions involved in the formation of Portland cement clinker suggest that fields should assist both the generation of active oxides from the raw components of the mix and their combination to form the various clinker phases. Consideration of the semiconductor properties of calcium oxide suggests that the formation of this compound from the calcium carbonate starting material could be enhanced under some conditions by field-dependent electrodesorption of CO_2 from the particle surfaces, and the dehydroxylation of kaolinite to form a reactive aluminosilicate is also known to be field-assisted. The observed effects of electric fields on the interoxide reactions involved in clinker formation can be explained in terms of a simple model which takes into account the relative diffusivities and electrical mobilities of the various ions, the oxygen packing of the matrices through which diffusion occurs, and the relative orientations of the reactant grains with respect to the field direction.

INTRODUCTION

In Part I of this paper[1], it was shown that the formation of Portland cement clinker phases is assisted by the application of d.c. electric fields. In this paper, an attempt is made to identify from theoretical considerations the processes by which electric fields act on the system.

DISCUSSION

The sequence of solid state reactions involved in the burning of Portland cement clinker consists of several stages, each of which may be separately influenced by electric fields. For convenience of discussion, two categories of reactions can be distinguished (a) the generation of active oxide reactants, and (b) the formation of products from these reactants. The effect of applied electric fields on both categories will now be considered.

Generation of reactants

The two reactions of interest here are the decarboxylation of calcium carbonate

$$CaCO_3 \xrightarrow{\sim 900\,°C} CaO + CO_2 \uparrow \tag{1}$$

and the dehydroxylation of kaolinite

$$Al_2O_3 \cdot 2\,SiO_2 \cdot 2\,H_2O \xrightarrow{500\text{–}600\,°C} Al_2O_3 \cdot 2\,SiO_2 + 2\,H_2O \xrightarrow{980\,°C} Si_3Al_4O_{12} + SiO_2 \tag{2}$$

Although no studies have been reported of the effect of electric fields on reaction (1), this reaction should be facilitated by electrolysis, since the diffusion of the gaseous product from the solid matrix should be assisted by the distorting effect of the field on the P.E. wells of the crystal lattice. The amount by which the height of the P.E. barrier is reduced in a field E is given by $Eea/2$, where e is the electronic charge and a is the separation of the P.E. well. Setting $a = 3$ Å, the energy barrier will be lowered by about 4×10^{-25} J in field of 10^5 V/m, i.e. the effect is very small at the present field strength. Nevertheless, the diffusion of uncharged species has been found in other cases to be facilitated by fields of similar magnitude, although the mechanism in these cases may be due to association of the neutral species with a charged species, and the "dragging" of the former by the latter[2].

There is, however, a second field-related effect which could affect the decarboxylation reaction. This is related to the modification of the electronic structure of semiconductor surfaces by electric fields, which change the surface potential. The resulting injection or removal of electrons from the surface states causes a bending of the valence and conduction bands either upwards or downwards, depending whether the surface potential is increased or decreased. The direction of bending of the bands is independent of whether the semiconductor is *p*- or *n*-type, although the degree of bending can be influenced by the type of semiconduction, which also determines whether the gaseous species will be adsorbed in the vicinity of an electron or hole at the semiconductor surface. The bonds involved in this type of absorption are usually described as "stable", with molecules thus adsorbed acquiring a formal charge. If the total number of adsorbed molecules per unit surface is N, with N^- of these having formed "stable" bonds, the fraction of these tightly bound species, η^-, is given by[3]

$$\eta^- = \{1 + \exp[(f^- - f^0 - F_0 - e\phi)/kT]\}^{-1} \tag{3}$$

where f^- and f^0 are the free energies of the polarised and unpolarised adsorbed molecules respectively, F_0 is the Fermi level of the semiconductor in the absence of a field and ϕ is the displacement of the edge of the semiconductor bands due to the field. In strong fields, ϕ can be approximately written as[3]

$$\phi = (\varepsilon kT/4\pi e^2 n^0)^{\frac{1}{2}} \exp\{[eE_0(\varepsilon kT/4\pi e^2 n^0)^{\frac{1}{2}}]/2kT\} \tag{4}$$

Where E_0 is the field strength and n^0 is the equilibrium concentration of charge carriers in the electrically neutral bulk of the semiconductor. Equations (3) and (4) confirm that the effect of an increasing electric field is to monotonically increase the proportion of strongly bound molecules up to a saturation value, at which $N^- = N$.

The total number of strongly bound molecules depends on the number of available electrons (or holes) in the surface states of the conduction band. The free electron concentration, n, is determined by the position of the Fermi level, since

$$F_0 - E_c = kT \ln(n/N_c) \tag{5}$$

where F_0 and E_c are the energies of the Fermi level and the bottom of the conduction band, respectively, and N_c is the number of available electron states at the bottom of the conduction band. Thus, in electric fields of positive polarity, or under oxidising conditions, de-electronation occurs, and the Fermi level is lowered. The degree of absorption of electron-accepting gaseous molecules is therefore decreased, and electrodesorption occurs at the surface (conversely, electroadsorption of electron-donating gaseous species should occur under these conditions). The reverse effect is predicted at negatively charged surfaces (or under reducing conditions). An interesting and relevant example of this phenomenon is the adsorption of CO_2 on tellurium[4], which is enhanced by negatively charging the surface, and decreased by positively charging the semiconductor. On the above reasoning, this suggests that the adsorbed species is, in this case, an electron acceptor; one such possible species would be CO, which might be formed by a shift to the right in the equilibrium

$$CO_2 \rightleftharpoons CO + 1/2\, O_2 \tag{6}$$

Although the band gap of tellurium at low temperatures (0.33 eV) and the electron populations of the conduction bands are rather different to the corresponding room-temperature parameters for CaO (bandgap = 7.7 eV)[5], it must be remembered that the temperature of the latter is 1000–1200°C in the present case. Since the probability that the conduction band energy levels, E_c, will be occupied by electrons [written $P(E_c)$] has the temperature dependence

$$P(E_c) = \frac{1}{\{1 + \exp[(E_c - F_0)/kT]\}} \tag{7}$$

it can be calculated from eqn. (7) that, from the point of view of electron distribution in the conduction band, CaO at 1200°C behaves similarly to a semiconductor with a bandgap of 1.6 eV at room temperature. Thus, it appears feasible that electroadsorption and electrodesorption might occur at the negative and positive faces, respectively, of CaO at higher temperature, on the basis of the above reasoning, and the experimental results for tellurium. This effect would lead to enhanced thermal decomposition at the positive electrode and a retarding effect at the negative electrode, and is consistent with the observed results[1].

The effect of electric fields on both the dehydroxylation of kaolinite[6] and the formation of the defect spinel phase[7] has previously been investigated, and both these reactions are known to be assisted by electric fields, their temperatures being, in some cases, lowered by as much as 60°C and 15°C, respectively, by electrolysis. Thus, in the present system, both reactions (1) and (2) should be facilitated by electric fields, but the effect in the electrode region will depend on the electrode polarity. In the case of kaolinite, the greatest degree of formation of the decomposition product occurs at the negative electrode, but the product formed at this electrode may be less reactive due to proton stabilization[7].

Solid state formation of product phases

After the reactants have been generated, a complex series of solid state reactions occurs. These include

(i) reactions between CaO and SiO_2[8]

$$2\,CaO + SiO_2 \xrightarrow{\sim 800\,^{\circ}C} Ca_2SiO_4 \tag{8}$$

$$Ca_2SiO_4 + CaO \xrightarrow{> 1200\,^{\circ}C} Ca_3SiO_5 \tag{9}$$

(ii) reactions between the aluminous component of the dehydroxylated kaolinite (written here as Al_2O_3 for simplicity) and CaO (ref. 9)

$$CaO + Al_2O_3 \xrightarrow{\sim 800\,^{\circ}C} CaAl_2O_4 \tag{10}$$

$$12\,CaO + 7\,Al_2O_3 \xrightarrow{800\text{–}900\,^{\circ}C} Ca_{12}Al_{14}O_{33} \tag{11}$$

$$Ca_{12}Al_{14}O_{33} + 9\,CaO \xrightarrow{\sim 1000\,^{\circ}C} 7\,Ca_3Al_2O_6 \tag{12}$$

(iii) reactions involving the Fe_2O_3 component of the raw mix[10]

$$2\,CaO + Fe_2O_3 \xrightarrow{\sim 800\,^{\circ}C} Ca_2Fe_2O_5 \tag{13}$$

$$Ca_2Fe_2O_5 + 2\,CaO + Al_2O_3 \xrightarrow{1100\text{–}1250\,^{\circ}C} Ca_4Al_2Fe_2O_{10} \tag{14}$$

At the temperatures of the present study, the formation of all these inter-oxide compounds involves inter-diffusion of ions in the reactant particles (diffusion in the liquid phase becomes important only above about 1260 °C, the temperature at which liquid first appears). As a starting point in discussing the effect of electric fields on these various interdiffusion processes, the relative importance of the diffusion of each species in the absence of a field will first be considered. An attempt will then be made to assess the effect of the field on the most significant diffusion processes.

Diffusion processes in the absence of a field. Since the present reactants are intimately mixed powders, the solid state reactions between them will involve the formation at the points of inter-particle contact of a product layer of increasing thickness with time, through which subsequent diffusion must occur[11]. Thus, the diffusion characteristics of the product as well as the reactant must be taken into account. Although inter-diffusion coefficients for all the oxide couples in the present system are not available in the literature, self-diffusion coefficients are available for

TABLE 1

DIFFUSION COEFFICIENTS AND ELECTRICAL MOBILITIES IN PURE OXIDES AT 1200 °C

Diffusing species	*D* (*cm^2 sec^{-1}*)	*μ* (*cm sec^{-1}/V cm^{-1}*)	*Ref.*
Ca in CaO	3.8×10^{-13}	8.97×10^{-10}	12
Al in Al_2O_3	3.4×10^{-16}	8.03×10^{-13}	13
O in Al_2O_3	1.7×10^{-16}	4.01×10^{-13}	14
Fe in Fe_2O_3	9.6×10^{-13}	2.27×10^{-9}	15
O in Fe_2O_3	1.8×10^{-11}	4.25×10^{-8}	16
O in SiO_2	3.8×10^{-13}	8.97×10^{-10}	17

TABLE 2

OXYGEN PACKING DENSITIES OF REACTANT AND PRODUCT PHASES IN CEMENT CLINKERING REACTIONS

Phase	*O packing density* (*g/cc*)	*Phase*	*O packing density* (*g/cc*)
SiO_2 (quartz)	1.41	C_3A	1.08
CaO	0.97	β-C_2S	1.22
Al_2O_3	1.87	C_4AF	1.23
$Si_8Al_{10\,2/3}\square_{5\,1/3}O_{32}$	1.31	C_3S	1.12 (mean)

most of the pure oxides of interest here. The relevant values at 1200 °C are tabulated in Table 1. The values of *D* for O in CaO and Si in SiO_2 are not at present available in the literature.

Since diffusion through the product phase becomes increasingly important as the reaction proceeds, it is of interest to estimate the relative ease with which this occurs in the various product phases. If the diffusing species are assumed to be cationic (this does not rule out anionic migration), then, according to Kohatsu and Brindley[9], the diffusibility is related to the oxygen packing of the anionic lattice (denser oxygen packing hinders cationic diffusion). Following Kohatsu and Brindley[9], the oxygen packing densities of the various reactant and product phases are shown in Table 2, in which the Al-containing reactant phase is more correctly considered as the defect spinel resulting from kaolinite decomposition, rather than pure Al_2O_3. The density data for the product phases were taken from Taylor[18], while the data for the Si–Al spinel were taken Rieke and Mauve[19].

Table 2 shows that on the basis of O packing densities, cationic diffusion should occur with almost equal facility in all of the product phases of interest, and, in addition, should occur more readily than in all of the reactant phases with the exception of CaO. Thus, the inter-diffusion rates should be determined, in general, by diffusion through the reactants rather than the products. From Table 1, it is seen that at

1200 °C, Ca diffuses more readily in CaO than does Al in Al_2O_3. Despite the somewhat denser oxygen packing in Al_2O_3 (Table 2), Ca has been experimentally shown[9] to diffuse preferentially into Al_2O_3 and not vice-versa. In the case of the CaO–SiO_2 couple, the diffusion rate of Ca in CaO is similar to that of O in SiO_2; although no data for Si diffusion are available, oxidation experiments suggest that Si diffuses much more slowly in SiO_2 than does oxygen (ref. 5, p. 349). On the basis of diffusivities, therefore, Ca would be expected to diffuse into SiO_2, as has been shown experimentally[20]. The slightly higher diffusion coefficient of iron (Table 1) suggests that the diffusion of this ion will not be the rate-limiting step in the formation of iron-containing phases.

Effect of electric fields on diffusion process. Although earlier workers appear to have assumed that the rates of diffusion processes are independent of applied electric fields, more recent work[21] has shown that electric fields do indeed facilitate ionic diffusion. Since a definite polarization effect was detected in the present results[1], such electrolytically assisted migration appears to be occurring here.

If an external electric field, E_0, is applied to ions migrating under diffusion conditions, the diffusion profile is shifted downfield by a distance Δ, given by[2]

$$\Delta = \mu_{\mathrm{eff}} E_0 t \tag{15}$$

where μ_{eff} is the effective mobility and is approximately equal to μ for monovalent ions in monovalent crystals. In more complex cases, such as pertain here, ion pairing of multivalent ions with vacancies can occur, but, for example, for divalent ions in monovalent crystals

$$\mu_{\mathrm{eff}} = \frac{\sigma_0}{\sigma} \mu \tag{16}$$

where σ_0 is the electrical conductance of the pure phase and σ is the conductance of the "doped" phase containing the foreign ion (in this case the product phase). Equation (15) shows that the effective shift in the diffusion profile is directly proportional to both the field strength and the time of its application. Such a simple relationship is not, however, observed in the present system because of the number of competing reactions which accompany the diffusion process. Equation (15) can be used to estimate the relative magnitude of the shifts in the diffusion profile for the various reaction couples in the present system provided μ_{eff} can be estimated. The electrical mobility, μ, of a species can be derived from the diffusion coefficient, D, for that species in the pure oxide via the Nernst–Einstein relation

$$\mu = \frac{De}{kT} \tag{17}$$

where e is the electronic charge and k is Boltzmann's constant. Values of electrical mobility thus derived are shown in Table 1. The effective mobilities of the appropriate species are then calculated from eqn. (16) by substituting conductivity data for the reactant and product phases[22] at the appropriate temperature (1200 °C). The effective

TABLE 3

CALCULATED SHIFTS OF DIFFUSION PROFILES FOR INTER-OXIDE CLINKER COMPOUNDS UNDER ELECTRIC FIELDS

Diffusion time = 7.2 × 10^3 sec; field strength = 2.0 × 10^3 V/cm.

Diffusion direction	*Product*	μ_{eff} *(cm sec^{-1}/V cm^{-1})*	Δ *(cm)*
Ca into Al_2O_3	C_3A	1.48×10^{-10}	2.13×10^{-3}
Al into CaO	C_3A	9.13×10^{-14}	1.31×10^{-6}
Ca into SiO_2	β-C_2S	1.68×10^{-10}	2.42×10^{-3}
Si into CaO	β-C_2S	3.77×10^{-13}*	5.43×10^{-6}
Ca into SiO_2	C_3S	4.12×10^{-10}	5.93×10^{-3}
Si into CaO	C_3S	9.24×10^{-13}*	1.33×10^{-5}
Fe into C_3A	C_4AF	5.19×10^{-9}	7.47×10^{-2}

* Based on an estimated mobility for Si in SiO_2 of 1×10^{-12} cm sec^{-1}/V cm^{-1}.

mobilities thus derived and the corresponding shifts in the diffusion profile are shown for the various reaction couples in Table 3.

It should be noted that, in the absence of self-diffusion data for Si in SiO_2, a value of μ for this species has been estimated on the basis that diffusion of Si in SiO_2 appears, from experiments on the oxidation of Si, to be at least two orders of magnitude slower than the diffusion of O in SiO_2 (see, for example, ref. 5, Chap. 14). The calculated values of Δ shown in Table 3 suggest that the formation of C_4AF from Fe_2O_3 and C_3A will be the most facilitated by electric fields. The formation of C_3S, β-C_2S and C_3A is affected less by electric fields, the magnitude of the effect being similar for all these phases. Table 3 also shows that when the direction of the field is contrary to the preferred diffusion direction for a particular couple, the field-induced shift of the diffusion profile is at least three orders of magnitude less than is the case when the field reinforces the preferred diffusion direction. All of these conclusions are in agreement with the observed experimental results, bearing in mind that at 1200°C C_3S is not a major phase, and that at this temperature other Ca-containing phases are readily formed at the expense of β-C_2S; the effect of electric fields on the concentration of both these phases is therefore less marked in practice than would be expected from Table 3.

The experimental observation of increased concentration of the alumina-containing phases C_3A and C_4AF at the positive electrode requires comment. This result is similar to that observed during the electrolysis of anhydrous MgO (ref. 23) and anhydrous TiO_2 (ref. 24). In these cases, the most mobile species were cationic, and it was suggested that their migration to the cathode eventually blocked further movement to that electrode. The migration of the less mobile oxide ions to the anode then became significant; these species recombined with the cations remaining at the anode to form a well-crystallized oxide phase. Such a mechanism is even more

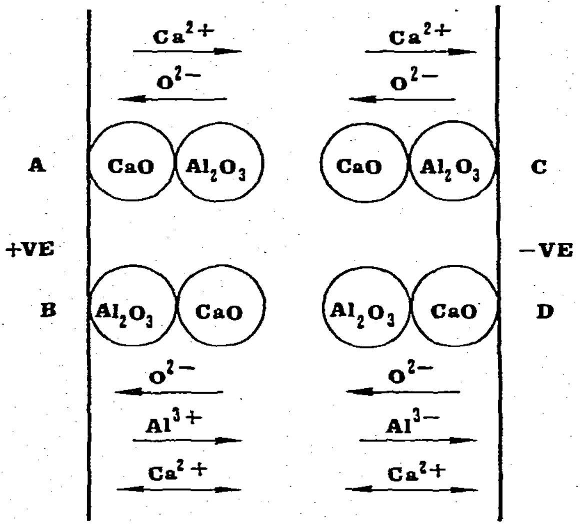

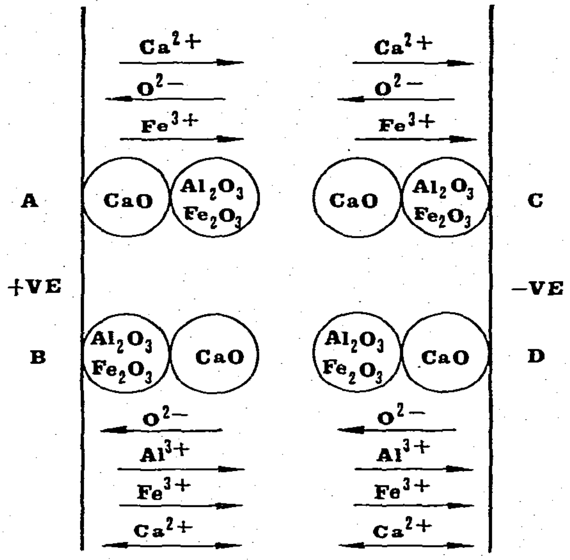

Fig. 1. Schematic diagram of a simplified model for solid state reaction between two oxide particles, showing ionic movements under an applied electric field for two extreme cases of grain orientation.

Fig. 2. Schematic diagram of a simplified model for solid state reaction between two oxides and a third component, showing ionic movements under an applied electric field for two extreme cases of grain orientation.

favourable in the present case, since at 1200°C, the mobilities of the relevant cations and anions are approximately equal (Table 1). A counter-migration of Ca^{2+} and O^{2-} during the solid-state reaction of CaO and Al_2O_3 has been suggested[9], and the concept of anion migration in oxide lattices is now generally accepted, particularly in polycrystalline systems[25].

Since the sample is composed of reactant particles of several different types in random orientation, a precise reaction model for the electrode processes cannot be proposed. It is possible, however, to gain a qualitative picture of the situation in the vicinity of the electrodes by considering a simplified case involving two reactants (say CaO and Al_2O_3), and treating the two extremes of particle orientation with respect to the field (Fig. 1). In this system, the diffusivity of Ca^{2+} is greater than that of Al^{3+}, and the diffusion direction in the absence of perturbations is Ca into Al_2O_3 (ref. 17). At the positive electrode (Fig. 1) when the reactants are ordered as in case A, the preferred diffusion direction is reinforced, and an increase in the rate of deposition of product layer will be observed. Some migration of Al^{3+} away from the reaction zone should also occur, but even in a field, the rate of this process is considerably less than the rate of Ca^{2+} entry into the reaction zone (Table 3). In the least favourable orientation (case B), the migration of Al^{3+} into CaO, although not preferred, should be slightly enhanced by the field. The Ca will, in this case, be subject to two opposing influences, namely, the normal thermal diffusion process tending to cause migration towards the electrode, and the field tending to cause a drift in the opposite direction. The nett effect is probably that the Ca undergoes relatively little displacement in either direction. Particles in orientations intermediate between these two extremes will behave in an intermediate fashion, and the observed result will represent an averaging over all the particles. At the negative electrode, the reverse situation occurs but with the added complication of the depletion of oxide ions and the accumulation, of cations, which subsequently block further migration. The overall effect is therefore that a higher concentration of better-crystallized product phase occurs at the positive electrode.

A similar model can be postulated for the binary system CaO–SiO_2 by substituting SiO_2 for Al_2O_3 in the previous argument.

The additional complication of a third component (say Fe_2O_3) can now be treated in an analogous manner (Fig. 2). Since, in practice, the Fe_2O_3 usually occurs in conjunction with the clay mineral, it is represented in Fig. 2 in intimate association with the aluminous phase. The diffusion coefficient and electrical mobility of Fe^{3+} are similar to Ca^{2+}, and significantly greater than those of Al^{3+}, so orientation A (Fig. 2) should result in the formation of less C_4AF at the positive electrode. On the other hand, orientation B, although not particularly favourable for C_3A, should be extremely favourable for C_4AF formation. Similar arguments can be applied to the negative electrode.

When considering the electrolytic behaviour of Fe^{3+}, account must also be taken of possible electrode reactions involving valency changes. Thus, at the negative electrode

$$Fe^{3+} + e^- \rightarrow Fe^{2+} \tag{18}$$

Such reactions are not necessarily undesirable in cement manufacture (firing the clinker in a reducing atmosphere is a well-known method of producing a white cement), but, for the purpose of the present phase analyses, this type of reaction could result in intensity changes in the X-ray pattern of the iron-containing phase and alter the analytical result.

CONCLUSIONS

Applied electric fields can influence the generation of active materials from a cement clinker raw mix. In addition to their known effect on the dehydroxylation of kaolinite, electric fields may also enhance the decomposition of calcium carbonate to the oxide, by influencing the rate at which the gaseous product is desorbed from the surface of the oxide grains. Theoretical considerations predict that this effect should occur at the positive electrode, in agreement with the experimental results.

Calculations on the inter-diffusion of the component oxides of the clinker phases under electric fields suggest that the formation of C_4AF is likely to be the most influenced by external fields due to the high electrical mobility of iron in this material. The calculations indicate that the formation of C_3A, C_3S and β-C_2S should be also influenced by electric fields, but to a lesser extent than C_4AF. These conclusions are qualitatively supported by the experimental results.

Variations in the content of the various clinker phases at the positive and negative electrodes can be accounted for by a simple model in which the relative orientations of the reactant grains with respect to the field direction are considered for two limiting cases.

REFERENCES

1 K. J. D. MacKenzie and R. A. Fletcher, *Thermochim. Acta*, 28 (1979) 161.

2 E. A. Kroger, *The Chemistry of Imperfect Crystals*, Vol. 3, North Holland, Amsterdam, 2nd edn., 1974, 25–33.

3 L. I. Ivankiv and A. M. Muzychuk, *Russ. J. Phys. Chem.*, 42 (1968) 223.

4 L. I. Ivankiv, A. M. Muzychuk and E. V. Solyanik, *Ukr. Fiz. Zhur.*, 14 (1969) 1227.

5 P. Kofstad, *Nonstoichiometry, Diffusion and Electrical Conductivity in Binary Metal Oxides*, Wiley–Interscience, New York, 1972, p. 127.

6 K. J. D. MacKenzie, *J. Therm. Anal.*, 5 (1973) 5.

7 K. J. D. MacKenzie, *Trans. J. Br. Ceram. Soc.*, 72 (1973) 209.

8 P. Fierens and P. Piquet, *J. Am. Ceram. Soc.*, 58 (1975) 50.

9 I. Kohatsu and G. W. Brindley, *Z. Phys. Chem.*, 60 (1968) 79.

10 See, for example, F. M. Lea and C. H. Desch, *The Chemistry of Cement and Concrete*, Arnold, London, 2nd edn., 1952.

11 W. Komatsu, in G. M. Schwab (Ed.), *Proc. 5th Symp. Reactivity of Solids*, Elsevier, Amsterdam, 1965, p. 182.

12 R. Lindner, St. Austrumdal and A. Akerstrom, *Acta Chem. Scand.*, 6 (1952) 468.

13 A. E. Paladino and W. D. Kingery, *J. Chem. Phys.*, 37 (1962) 957.

14 Y. Oishi and W. D. Kingery, *J. Chem. Phys.*, 33 (1960) 480.

15 R. Lindner, *Ark. Kemi*, 4 (1952) 381.

16 W. D. Kingery, D. C. Hill and R. P. Nelson, *J. Am. Ceram. Soc.*, 43 (1960) 473.

17 E. W. Sucov, *J. Am. Ceram. Soc.*, 46 (1963) 14.

18 H. F. W. Taylor, *The Chemistry of Cements*, Vol. 2, Academic Press, London, 1964, pp. 348–404.

19 R. Rieke and L. Mauve, *Ber. Dtsch. Keram. Ges.*, 23 (1942) 119.

20 (a) H. Tagai, T. Iseki, T. Sakei and T. Kounosu, *Yogyo Kyokai Shi*, 77 (1969) 341. (b) R. Hayami and T. Ogara, *Osaka Kogyo Gijutsu Shikensho Kiho*, 20 (1969) 270.

21 M. Arnikar and R. Chaure, *Proc. Chem. Symp. Chandigarh*, Vol. 2, 1969, p. 144.

22 K. J. D. MacKenzie, *Trans. J. Br. Ceram. Soc.*, 77 (1978) 13.

23 K. J. D. MacKenzie and P. J. Melling, *Thermochim. Acta*, 9 (1974) 389.

24 K. J. D. MacKenzie, R. Smits and P. J. Melling, *Trans. J. Br. Ceram. Soc.*, 73 (1974) 185.

25 A. E. Paladino and R. L. Coble, *J. Am. Ceram. Soc.*, 46 (1963) 133.